Classical and semi-classical treatments of Li^{3+}, Ne^{10+} + H(1s) collisions

L. F. Errea, Clara Illescas, L. Méndez, B. Pons†, A. Riera and J. Suárez

Laboratorio Asociado al CIEMAT de Física Atómica y Molecular en Plasmas de Fusión,
Departamento de Química C-IX, Universidad Autónoma, 28049 Madrid, Spain
† Centre Lasers Intenses et Applications, UMR 5107 du CNRS,
Université de Bordeaux-I, 351 Cours de la Libération, 33405 Talence, France

Abstract. We perform molecular close-coupling and impact-parameter classical trajectory Monte-Carlo calculations of total and partial cross sections for capture and ionization in collisions of highly charged ions on H(1s). We first consider Li^{3+}+H(1s) as a benchmark to ascertain the complementarity of the methods, and then Ne^{10+}+H(1s), which has been scarcely studied up to now, and has recently become of interest for fusion plasma research.

PACS numbers: 34.10.+x

1. Introduction

Collisional processes are of paramount importance in the dynamics of thermonuclear fusion plasmas. They play a critical role in the initiation of the plasma from the neutral gas and in the control of plasma density and composition. Further, several diagnostics based on atomic and molecular processes have been implemented for edge and core plasma characterization. For instance, the charge state, temperature, and density of ionic impurities in tokamak devices are frequently obtained by charge exchange spectroscopy (CXS) (Isler 1994). A neutral beam (D or He) is injected into the plasma and the spectroscopic diagnostic consists in analyzing the radiative decay of the excited states formed by electron capture from the neutral atoms of the beam by the impurity ions. Accurate partial cross sections for the underlying charge transfer processes have thus to be known, and in these applications, an accuracy of 20-25% of state selective charge transfer cross sections is usualy required (Folkerts *et al* 1994, Hoekstra *et al* 1998). Chemical species with nuclear charges $Z \leq 8$ are currently found in the plasmas of operating tokamak machines; these impurities are mainly desorbed from the coated walls and become progressively stripped as they approach the inner region of the plasma. The energies of the neutral beams are typically in the range of 10 to 100 keV/amu, that encompasses the maximum of ionization cross sections in A^{Z+} + H, He, H_2

collisions with $1 \leq Z \leq 8$. During the past decades, many experimental and theoretical works have filled in many gaps in the collisional databases (Janev 1989, Janev 1996). Nevertheless, much more work is required to support the recent advances of tokamak technology; indeed, it has been observed in the larger devices worldwide (Ongena *et al.* 2001, Esipchuk Yu V. *et al.* 2003) that energy and/or particle confinement is greatly improved by seeding (very) highly charged impurities (Ne, Ar) in the plasma edge (Tokar *et al* 2000). CXS diagnostics and plasma modeling thus give the impetus to establishing a comprehensive cross section database for the collision processes involving these highly charged ions.

In the present contribution, we will focus on charge transfer and ionization processes in Ne^{10+}+H(1s) collisions, which are actually employed in CXS experiments in ASDEX-U. To our knowledge, this system has only been experimentally studied in the Oak Ridge measurements (Meyer *et al* 1985*a*, Meyer *et al* 1985*b*) for total electron capture. Classical Trajectory Monte Carlo (CTMC) calculations have been carried out by Olson and Salop (1977), Olson (1981), Perez *et al* (2001), Maynard *et al* (1992) and Schultz and Krstić (1996). One can collect from these calculations total cross sections for $E \leq 1000$ keV/amu and some partial (n, l) capture ones up to $n = 7$ and $E = 200$ keV. Nevertheless, the Ne^{10+}+H collisional database still remains far from being complete with respect to the needs of fusion research; in particular, cross sections for charge transfer into higher n levels and associated (n, l) subshells are required. Besides, the accuracy of the computed CTMC cross sections has never been thoroughly checked, especially at low E. Therefore, we use both the semi-classical molecular (Harel *et al* 1998) and classical impact-parameter CTMC (Illescas *et al* 1998, Illescas and Riera 1999) methods to provide total and partial cross sections for capture and ionization over a wide range of impact energies, $1 \leq E \leq 500$ keV/amu. The former approach is known to be well suited to the low energy region (Harel *et al* 1998); a representation of the ionization channel by means of mid-centered pseudostates allows to extend its validity up to the intermediate velocity range where the ionization cross section is maximal (Errea *et al* 1998*a*). CTMC calculations, with improved initial conditions and large statistics, are more appropriate from intermediate to high impact energies (Illescas and Riera 1999). We thus shall combine both methods to accurately evaluate cross sections over (and beyond) the entire domain of interest for fusion plasma research. Nonetheless, because of the scarcity of experimental and theoretical data for such highly charged projectiles as Ne^{10+}, we shall first ascertain the reliability and complementarity of our methods in the case of Li^{3+}+H(1s) collisions, which have been studied in many theoretical and experimental works.

The paper is organized as follows: in section 2, we set out the main equations of the impact parameter molecular and CTMC formalisms; we then present in section 3 the total and partial cross sections obtained for Li^{3+} and Ne^{10+} collisions with H(1s) and draw our conclusions and future plans in section 4. Atomic units are used throughout unless explicitly stated.

2. Impact parameter molecular and CTMC methods

The two approaches are based on the impact parameter approximation (Bransden and McDowell 1992), in which the projectile follows rectilinear trajectories with constant velocity $\boldsymbol{v}$ and impact parameter $\boldsymbol{b}$. This classical treatment of the nuclear motion is justified in the impact energy range considered ($E \geq 1$ keV/amu) because of the heavy mass of the projectiles; deviations from linear trajectories generally become significant for $E \leq 250$ eV/amu (Errea *et al* 1998*b*, Le *et al* 2004).

2.1. The molecular close-coupling formalism

For each nuclear trajectory (v, b), the internuclear vector $\boldsymbol{R}$ evolves as $\boldsymbol{R}(t) = \boldsymbol{b} + \boldsymbol{v}t$ and the electronic motion is quantum mechanically described by the time-dependent Schrödinger equation:

$$(H - i\partial)\Psi(\boldsymbol{r}, v, b, t) = 0 \tag{1}$$

where H is the (fixed-nuclei) Born-Oppenheimer Hamiltonian associated to the one-electron problem A^{Z+}+H(1s):

$$H = -\frac{1}{2}\nabla^2 - \frac{Z}{r_A} - \frac{1}{r_H} \tag{2}$$

and $\boldsymbol{r}_{A,H}$ are the electron position vectors relative to nuclei A^{Z+} and H^+. ∂ is the time derivative taken by keeping fixed the electron position vector $\boldsymbol{r}$ with respect to an origin of coordinates that is situated on the internuclear axis at distances pR and qR from the target and projectile nuclei, respectively ($p + q = 1$).

In standard molecular treatments, eq. (1) is solved by expanding Ψ in terms of bound eigenfunctions χ_k of the electronic Hamiltonian H:

$$H\chi_k(\boldsymbol{r}, R) = E_k(R)\chi_k(\boldsymbol{r}, R). \tag{3}$$

These eigenfunctions are called one-electron diatomic molecule (OEDM) orbitals (Power 1973), and are asymptotically correlated as $R \to \infty$ to the capture and excitation atomic states $\phi_{nlm}^{A,H}(\boldsymbol{r})$. Ψ is thus given by:

$$\Psi(\boldsymbol{r}, v, b, t) = e^{iU(\boldsymbol{r},t)} \sum_k a_k(v, b, t)\chi_k(\boldsymbol{r}, R)e^{-i\int_0^t E_k(t')dt'} \tag{4}$$

where $U(\boldsymbol{r}, t)$ is a common translation factor (CTF), introduced to account for the momentum transfer problem (Schneiderman and Russek 1969, Errea *et al* 1994), and is of the form:

$$U(\boldsymbol{r}, t) = f(\boldsymbol{r}, t)\boldsymbol{v} \cdot \boldsymbol{r} - \frac{1}{2}f^2(\boldsymbol{r}, t)v^2 t \tag{5}$$

with

$$f(\boldsymbol{r}, t) = \frac{1}{2}(g_\alpha(\mu) + d) \tag{6}$$

and

$$g_\alpha(\mu) = \alpha^{\alpha/2}\frac{\mu}{(\alpha - 1 + \mu^2)^{\alpha/2}} \tag{7}$$

where $d = 1 - 2p$ and $\mu = (r_H - r_A)/R$ is the prolate spheroidal coordinate. As in previous calculations (Errea *et al* 1992, Errea *et al* 1996), the parameter α is chosen by checking the stability of the computed cross sections with respect to its variation; in what follows, $\alpha = 1.25$ for all cases.

Substitution of the ansatz (4) in Eq. (3) leads to a set of differential equations for the expansion coefficients $a_k(v, b, t)$,

$$\frac{\mathrm{d}a_k(v,b,t)}{\mathrm{d}t} = \sum_j a_j(v,b,t) \left(\left\langle \chi_k \left| -\frac{\partial}{\partial t} \right| \chi_j \right\rangle - \mathrm{i} \left\langle \chi_k \left| \frac{1}{2}(\nabla U)^2 + \frac{\partial U}{\partial t} \right| \chi_j \right\rangle + \right.$$
$$\left. + \left\langle \chi_k \left| -\frac{1}{2}\nabla^2 U - \nabla U \cdot \nabla \right| \chi_j \right\rangle \right) \exp\left[-i \int_0^t (E_j(t') - E_k(t')) \mathrm{d}t' \right] \tag{8}$$

which is numerically integrated up to time t_{max}. One next obtains the capture and excitation transition amplitudes $a^{A,H}_{nlm}(v, b, t \to \infty)$ by projecting Ψ onto the atomic scattering states at time t_{max}, and by applying the extrapolation procedure proposed in (Salin 1984), that accounts for the Stark effect and the residual rotation of the internuclear axis from t_{max} to infinity:

$$a^{A,H}_{nlm}(v,b,t\to\infty) = \sum_{m'} < \phi^{A,H}_{nlm} | \mathcal{R} | \phi^{A,H}_{nlm'} > \sum_k a_k(v,b,t_{max}) \tag{9}$$
$$< \phi^{A,H}_{nlm'} | \chi_k > \exp\left(-i f_k(t_{max}) - i \int_0^{t_{max}} E_k(t') \mathrm{d}t' + i \int_0^{\infty} \epsilon_{nlm} \mathrm{d}t' \right)$$

with

$$f_k(t_{max}) = \frac{Q < \chi_k | \boldsymbol{r} \cdot \hat{\boldsymbol{R}} | \chi_k >}{bv} \tan^{-1} \frac{b}{v t_{max}} \tag{10}$$

where $Q = 1$ and Z for capture and excitation channels respectively, and $\mathcal{R}$ is the rotation operator connecting the spherical hydrogenic state $\phi^{A,H}_{nlm'}$ defined in the rotating molecular frame at time t_{max} (with the quantization axis along the internuclear direction $\hat{\boldsymbol{R}}$) and the asymptotic atomic state $\phi^{A,H}_{nlm}$ (with corresponding eigenvalue ϵ_{nlm}). Then, finally, the cross section to a specific final (n, l, m) state is given by:

$$\sigma^{A,H}_{nlm}(v) = 2\pi \int |a^{A,H}_{nlm}(v,b,t\to\infty)|^2 b \mathrm{d}b. \tag{11}$$

The two-center effects that govern the dynamics of all the inelastic processes in low energy ion-atom collisions are naturally well represented by the OEDM orbitals. In close-coupling atomic calculations, pseudo-continuum states are usually required to improve the description of the two-center nature of the electronic wavefunctions (Bransden and McDowell 1992, Fritsch and Lin 1982). This is particularly true for highly charged projectiles where convergence problems related to the pseudostate sets can appear. However, standard molecular expansions do not include an explicit representation of the ionization channel; the variational character of the method and the dynamical properties of the (fixed-nuclei) molecular orbitals then lead to an accumulation of the ionizing flux on the highest levels introduced in the expansion (Errea *et al* 1992, Harel *et al* 1997). This is of no inconvenience insofar as ionization is negligible, *i.e.* in the low impact energy regime $E \lesssim 10$ keV/amu. At the threshold of the intermediate domain

$10 \lesssim E \lesssim 50$ keV/amu, where ionization starts to be sizeable, a practical procedure consists in adding higher capture or excitation channels to the molecular basis set in order to ensure that the trapping of the ionization flux does not affect the computed cross sections for capture into low-lying levels (Harel *et al* 1998, Errea *et al* 1992). The use of a triple-centre basis, in terms of OEDM orbitals augmented with a set of mid-centered pseudostates, allows to extend the validity of the molecular approach to even higher energies and to explicitly evaluate the ionization cross section (Errea *et al* 1998*a*). These pseudostates are located at a distance gR of the target and are Gaussian functions of the form:

$$\mathcal{G}(\boldsymbol{r}) = x^{n_1}(z + (p-g)R)^{n_2} e^{-\gamma_n r_g^2} \tag{12}$$

with

$$r_g^2 = x^2 + y^2 + (z + (p-g)R)^2 \tag{13}$$

where x, y, z are the electronic coordinates in the rotating molecular frame, with z along the internuclear axis and y perpendicular to the collision plane (x, z). The parameter γ_n are in geometrical series:

$$\gamma_n = \gamma_0 \beta^n. \tag{14}$$

The third-centre basis is thus defined by the parameters g, γ_0, β, n_{max} such that $0 \leq n \leq n_{max}$ and L_{max} such that $0 \leq n_1 + n_2 \leq L_{max}$. The sum of the pseudostate populations provides the exit ionization probability and the corresponding cross section is obtained, according to (11), by integration over the impact parameter.

2.2. The impact parameter CTMC formalism

For each nuclear trajectory (v, b), the electron dynamics is described through a set of N independent trajectories $\{\boldsymbol{r}_j(t)\}$ whose statistical phase-space distribution

$$\rho(\boldsymbol{r}, \boldsymbol{p}, v, b, t) = \frac{1}{N} \sum_{j=1}^{N} \delta(\boldsymbol{r} - \boldsymbol{r}_j(t)) \delta(\boldsymbol{p} - \boldsymbol{p}_j(t)) \tag{15}$$

satisfies the Liouville equation

$$\frac{\partial \rho(\boldsymbol{r}, \boldsymbol{p}, v, b, t)}{\partial t} = -[\rho(\boldsymbol{r}, \boldsymbol{p}, v, b, t), H]. \tag{16}$$

Standard CTMC treatments employ the microcanonical distribution

$$\rho(\boldsymbol{r}, \boldsymbol{p}, v, b, t \to -\infty) = \frac{1}{8\pi^3} \delta(\frac{p^2}{2} - \frac{1}{r} + \frac{1}{2}) \tag{17}$$

to describe the initial H(1s) state (Abrines and Percival 1966, Olson and Salop 1977). This distribution yields a momentum density identical to the quantal one, but its spatial density is too compact, with a cutoff value at $r = 2$ a_0. Hardie and Olson (1983) thus proposed to improve the description of the spatial density (without damaging seriously

the momentum one) by using a hydrogenic distribution, defined as superposition of $\mathcal{N}$ microcanonical functions:

$$\rho(\boldsymbol{r},\boldsymbol{p},v,b,t\rightarrow-\infty)=\sum_{k=1}^{\mathcal{N}}\frac{(-2\mathcal{E}_k)^{5/2}}{8\pi^3}\,a_k\,\delta\left(\frac{p^2}{2}-\frac{1}{r}-\mathcal{E}_k\right) \tag{18}$$

where the energies $\mathcal{E}_k$ and weights a_k are chosen so as to achieve good approximations to the quantum densities. The substitution of eq. (15) in (16) yields the Hamilton equations:

$$\dot{\boldsymbol{r}}_j(t)=\frac{\partial H}{\partial\boldsymbol{p}_j(t)}\qquad\dot{\boldsymbol{p}}_j(t)=-\frac{\partial H}{\partial\boldsymbol{r}_j(t)} \tag{19}$$

for the temporal evolution of the N independent trajectories, that are integrated up to time t_{max}. The ionizing part ρ_i of the classical distribution is obtained at the end of the collision under the atomic energy conditions $\{E_T=\boldsymbol{p}^2/2-1/r>0, E_P=1/2(\boldsymbol{p}-\boldsymbol{v})^2-Z/|\boldsymbol{r}-\boldsymbol{b}-\boldsymbol{v}t_{max}|>0\}$ while for the capture part ρ_c, $\{E_T>0, E_P<0\}$. Moreover, the classical phase space of the capture electrons is partitioned into exclusive subspaces, each of them being associated with a quantum state with definite n and l. The partition is made so that the relative volume of a given subspace matches the multiplicity of the corresponding quantum shell (Becker and MacKellar 1984); all the electronic trajectories which end up with an energy $E_P=-Z^2/2n_c^2$ and an angular momentum $l_c=|(\boldsymbol{r}-\boldsymbol{b}-\boldsymbol{v}t_{max})\wedge(\boldsymbol{p}-\boldsymbol{v})|$ relative to the projectile such that:

$$\left[\left(n-\frac{1}{2}\right)(n-1)n\right]^{1/3}<n_c\leq\left[n\left(n+\frac{1}{2}\right)(n+1)\right]^{1/3},$$
$$l<\frac{n}{n_c}\,l_c\leq l+1 \tag{20}$$

are accordingly taken to belong to the (n,l) quantum state. The classical ionization $\mathcal{P}_i^C$ and capture $\mathcal{P}_{c_{(n,l)}}^C$ probabilities are then calculated

$$\mathcal{P}_{i,c_{(n,l)}}^C(v,b)=\int\mathrm{d}\boldsymbol{r}\int\mathrm{d}\boldsymbol{p}\rho_{i,c_{(n,l)}}(\boldsymbol{r},\boldsymbol{p},v,b,t_{max}) \tag{21}$$

to provide the cross sections by numerical integration over the impact parameter (11).

3. Results

3.1. Li^{3+}+H(1s) collisions

We have performed close-coupling calculations in the impact energy range $1\leq E\leq 100$ keV/amu by employing two molecular basis sets: a conventional one (P88) which includes all the 88 OEDM orbitals correlating to excitation and capture channels up to $n=2$ and 7, respectively, and a triple-center basis (P35+$\mathcal{G}$), which consists of the 35 OEDM's with $m\leq 2$ associated to the most important $n=1-2$ excitation and $n=1-5$ capture manifolds, to which we have added a gaussian set $\{\mathcal{G}\}$ (Eq. (12)), defined by $g=0.5$, $\alpha_0=0.03$, $\beta=2.5$, $n_{max}=4$ and $L_{max}=5$. For $(n_1=0,n_2)$,

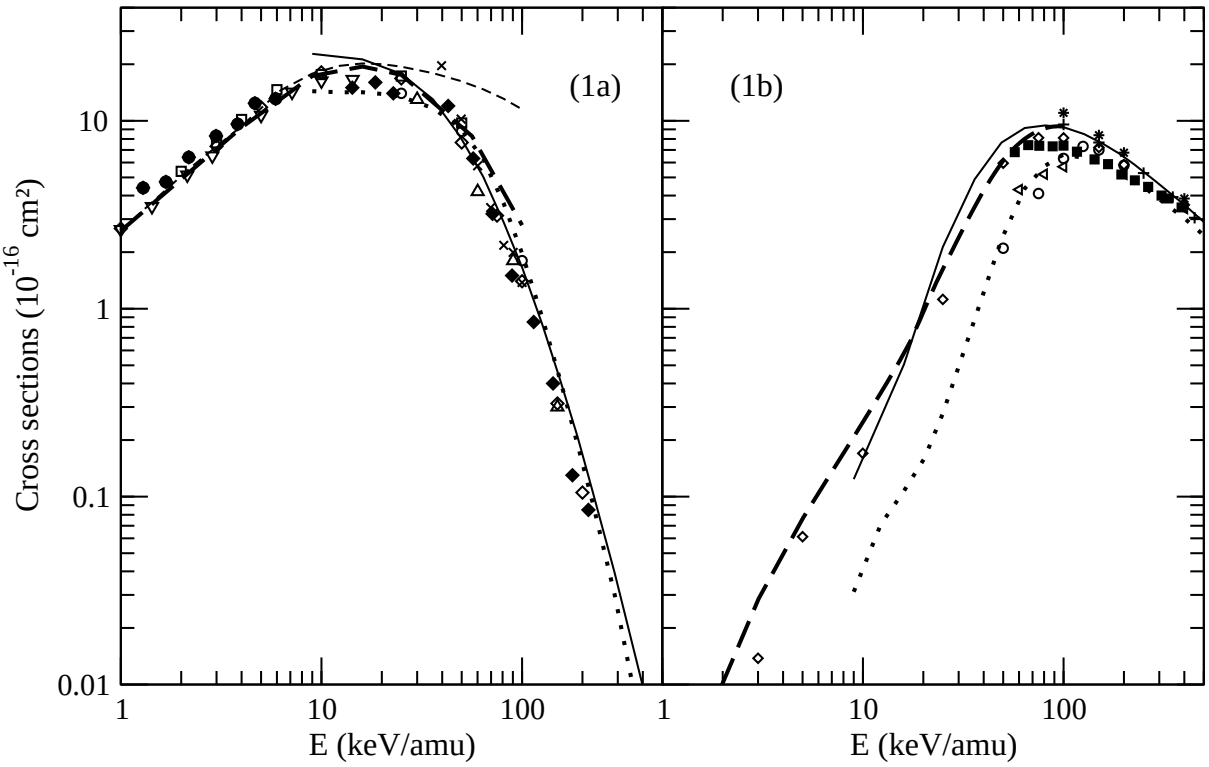

Figure 1. Total capture (1a) and ionization (1b) cross sections in Li^{3+}+H(1s) collisions, as a function of the impact energy E. P88 (dashed line) and P35+$\mathcal{G}$ (long-dashed line) present molecular results; present CTMC results: microcanonical (....), hydrogenic (——) ; experimental data for capture: (•) (Seim *et al* 1981), (⧫) (Shah *et al* 1978), and ionization (■) (Shah and Gilbody 1982); other theoretical data: AO+ (▽) (Fritsch and Lin 1982), Hylleraas (□) (Lüdde and Dreizler 1982), 2CAO (◊) (Toshima 1994, Toshima 1997) close-coupling expansions; STO (+) (Martín 1999) and spherical Bessel (∗) (Sevila 2003) monocentric expansions; three-body CTMC (◯) (Olson and Salop 1977) results; perturbative CDW (×) (Belkič *et al* 1992), EI (△) (Gravielle and Miraglia 1995) and CDW-EIS (◁) (Crothers and McCann 1983) results.

we have restricted the geometrical series (14) to its lowest term, to avoid quasilinear dependences in the basis.

CTMC calculations with the microcanonical and hydrogenic distributions have been carried out using respectively $N = 30000$ and 40000 electronic trajectories. Classical cross sections are reported for $9 \leq E \leq 500$ keV/amu.

In Fig. 1a, we compare our total capture cross sections to the experimental data of Seim *et al* (1981) and Shah *et al* (1978). Both experiments used a beam-static gas target approach and determined the fractional yield of Li^{2+} ions through an electrostatic (Shah *et al* 1978) or magnetic (Seim *et al* 1981) analysis of the charge state population of the emergent beam. We also include in this figure the two-center atomic orbital (2CAO) close-coupling expansions of Toshima (1994) and Fritsch and Lin (1982). While the 2CAO basis of Toshima (1994) includes a large number of target- and projectile- centered pseudostates, the basis set of Fritsch and Lin (1982) (AO+ expansion) is restricted to

the main bound channels, to which they added united-atom (Be^{3+}) orbitals to improve the description of the molecular binding effect in slow collisions. Lüdde and Dreizler (1982) used an alternative to these atomic treatments, in terms of prolate spheroidal Hylleraas wavefunctions. For high impact energies, Gravielle and Miraglia (1995) and Belkič *et al* (1992) employed respectively the perturbative eikonal impulse (EI) and continuum distorted wave (CDW) approaches. Finally, Olson and Salop (1977) applied the three body CTMC with the microcanonical distribution (17) to describe the initial H(1s) state.

Our molecular P88 and P35+$\mathcal{G}$ results nicely agree at $E < 25$keV/amu with both the measurements of Seim *et al* (1981) and the other close-coupling calculations. The P88 expansion, in terms of bound OEDM orbitals only, does not describe the fall of the charge exchange cross section in the intermediate regime $E \gtrsim 25$ keV/amu; as explained above and found in our previous studies of multicharged ion-atom collisions (Harel *et al* 1997), the computed total capture cross section rather closely corresponds to the sum of the genuine capture and ionization cross sections. On the other hand, the classical approximation is not able to describe the decreasing shape of the charge exchange cross section before its maximum, approximately located at $E = 20$ keV/amu, but leads for $E \geq 25$ keV/amu to accurate results in good agreement with the experimental data of Shah *et al* (1978) and with the EI and CDW perturbative cross sections. The CTMC and standard molecular treatments thus suitably complement each other at the threshold of the intermediate energy range ($E \simeq 25$eV/amu). The overlapping region of our classical and semi-classical results is even enlarged when mid-centered Gaussian pseudostates are included in the molecular expansion; the capture and ionization contributions to the target electron-loss process are then unambiguously separated and the P35+$\mathcal{G}$ capture cross section exhibits the correct behavior up to $E \simeq 60$ keV/amu. Within classical treatments, the microcanonical (17) and hydrogenic (18) initial distributions lead to almost indistinguishable capture cross sections for $E \geq 100$ keV/amu; at lower energies, the microcanonical results depart from the other ones and tend to underestimate, for $E \leq 30$ keV/amu, the total capture cross section. In this energy range, the inelastic processes mainly occur through long-range transitions that involve the outer part of the target-centered electronic cloud, and are consequently inhibited when one uses the too compact microcanonical distribution (17) with $\mathcal{E} = -0.5$ a.u..

This liability appears to be enhanced in the case of ionization, as shown in Fig. 1b, where we display our P35+$\mathcal{G}$ and classical ionization cross sections as functions of E. The microcanonical initial distribution yields a cross section underestimated by one order of magnitude at the lowest energies, and this results in a misplaced maximum located about $E \sim 125$ keV/amu. The agreement of the microcanonical CTMC cross section with the results of Crothers and McCann (1983) at $E \leq 100$keV/amu is probably fortuitous, since these are very low energies to apply perturbative methods. The CMTC cross section with hydrogenic initial distribution shows good agreement with both molecular and 2CAO (Toshima 1994) atomic results, which maximize around $E \sim 85$ keV/amu, and the shapes are similar to that of the experimental data of

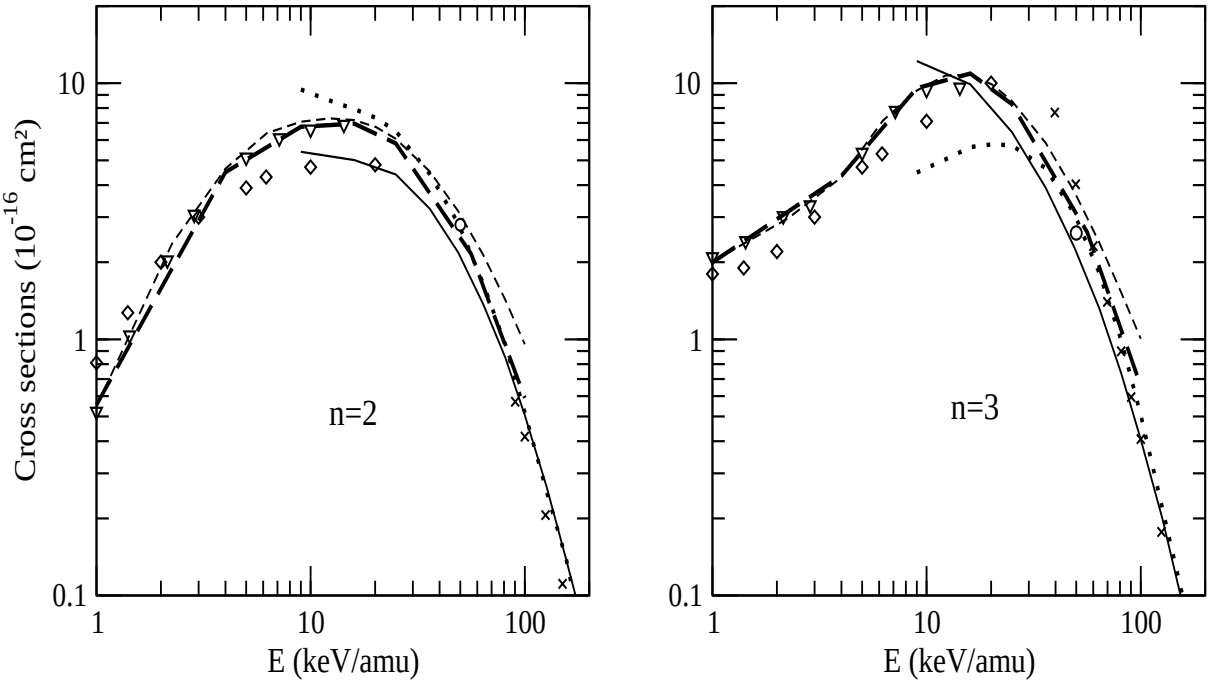

Figure 2. Cross sections for the reactions Li^{3+}+H(1s) $\longrightarrow$ $Li^{2+}(n)$+H^+, as a function of the impact energy E. Same symbols as in Fig. 1.

Shah and Gilbody (1982), obtained by using a crossed-beam setup and merging time-of-flight spectroscopy and coincidence techniques to characterize the ionizing collisions. Nevertheless, the measured values are $\sim$ 20% smaller than our theoretical ones; this might be due to the normalization procedure of the experimental data (see Toshima (1999)). However, this possibility appears to be ruled out by the good agreement (see fig. 1b) of the experimental ionization cross section with those supplied by the monocentric calculations of Martín (1999) and Sevila (2003), the CDW-EIS of Crothers and McCann (1983), and the present CTMC results for $E \geq 100$ keV/amu, which accurately tend to the Born limiting values used in the normalization procedure. The origin of the experimental/theoretical discrepancy on the ionization cross section around its maximum thus remains an open question. Nonetheless, the striking agreement of all theoretical calculations cannot be coincidental, and gives the impetus to further experimental investigations. Finally, one can verify in Figs. 1, by comparing our classical cross sections with those of Olson and Salop (1977), that three-body and impact-parameter CTMC calculations yield similar cross sections provided that the initial distributions are the same.

To further compare molecular and CTMC methods, we present in Fig. 2 the partial cross sections for capture into Li^{2+}(n=2,3)+H^+. In the low velocity regime, our molecular results are in excellent agreement with the AO+ results of Fritsch and Lin (1982), and the accord with the 2CAO cross sections of Toshima (1997) is also satisfactory. Within molecular calculations in terms of bound orbitals only, the

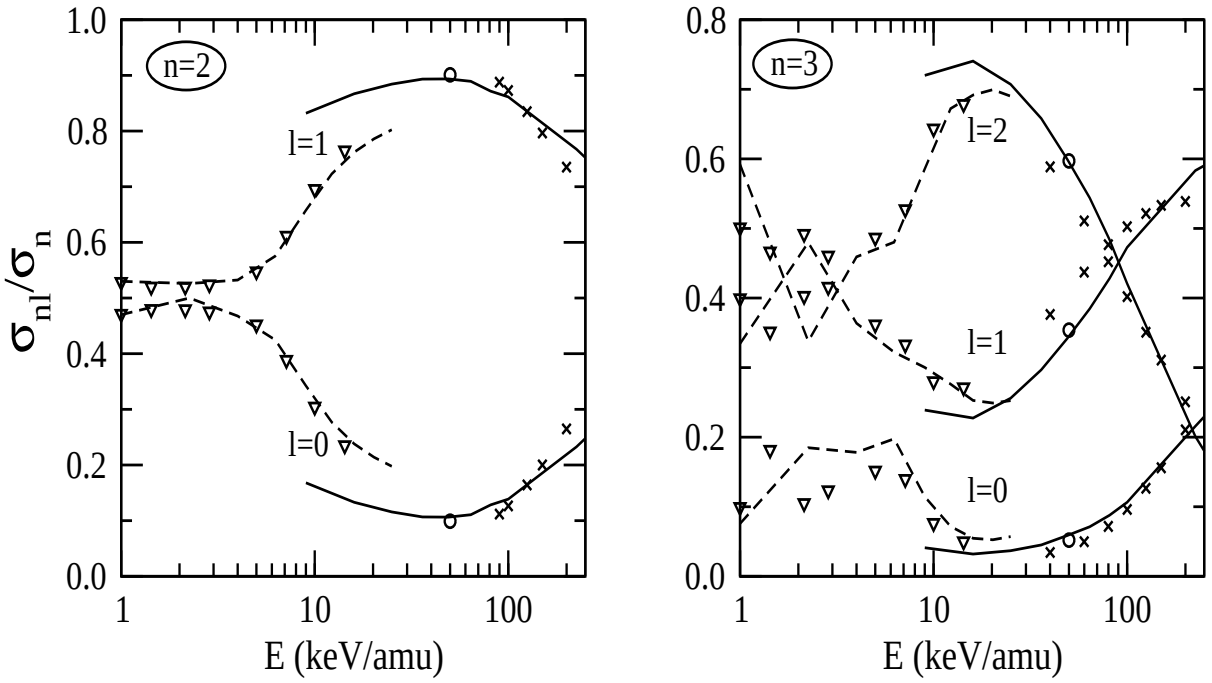

Figure 3. l-contributions to the partial n-capture cross sections in Li^{3+}+H(1s) collisions, illustrated through the ratios σ_{nl}/σ_n as a function of the impact energy E. Same symbols as in Fig. 1.

accumulation of the ionization flux finally ends up in the highest manifolds introduced in the expansion (Errea *et al* 1992, Harel *et al* 1997); we consequently obtain, by means of the P88 calculations, well-behaved cross sections for the lower capture channels up to $E = 100$ keV/amu. It can be checked in Fig. 2 that the remaining contamination of these capture populations by the ionizing flow is very small by comparing P88 and P35+$\mathcal{G}$ results. Although the agreement is somewhat less satisfactory than for the total capture cross sections (fig. 1a), close-coupling molecular cross sections and CTMC partial cross sections can be joined at $E \simeq 30$keV/amu. Besides, the CTMC calculation closely reproduces the CDW data of Belkič *et al* (1992) for $E \geq 70$ keV/amu, thus supporting the validity of this method at high impact energies. The use of the $\mathcal{E} = -0.5$ a.u. microcanonical distribution is adequate only in the high impact energy range ($E > 50$keV/amu), but it leads to a significant underestimation of the maximum of the cross sections for the highest capture channels.

The l-contributions to the partial n cross sections are displayed in Fig. 3, where we have plotted the ratios σ_{nl}/σ_n, with $n = 2, 3$ and $0 \leq l \leq n-1$, as functions of the impact energy E. Our P88 molecular results nicely agree with the AO+ simulations of Fritsch and Lin (1982) for $E \leq 25$ keV/amu. Both sets of results suitably merge in the intermediate impact velocity range, where the three-body CTMC calculations of Olson and Salop (1977) yield identical results than our impact-parameter ones.

As a practical conclusion of our calculations for electron capture in Li^{3+}+H(1s)

collisions, close-coupling (with a large basis of bound molecular orbitals) and CTMC methods yield total and partial cross sections for the dominant channels that smoothly join at impact energies ($E \simeq 30$ keV/amu in this case) near the ionization threshold, provided that an improved initial distribution is employed in the CTMC calculation. The ionization cross section can be accurately calculated at low impact energies by adding pseudostates to the molecular basis, but these pseudostates are not required to evaluate capture cross sections at low v unless one is interested in the populations of high-lying bound states, which can be considerably contaminated by the ionization flux. On the other hand, at high energies ($E \simeq 75$keV/amu), the CTMC calculation with the hydrogenic initial distribution agrees with accurate calculations in this region: perturbative (CDW) calculations of total and partial capture cross sections, and perturbative (CDW-EIS) and monocentric expansions for ionization.

3.2. Ne^{10+}+H(1s) collisions

Our molecular treatment employs 213 OEDM orbitals, correlated to the entry channel and to the $n = 4 - 11$ capture manifolds. The description of the $n = 10, 11$ channels has been restricted to the states with $m \leq 2$. According to our previous conclusions, we have performed dynamical molecular calculations up to the intermediate regime, $E \simeq 50$ keV/amu, and did not undertake calculations including pseudostates, since these latter are too prone to linear dependences with so many bound orbitals. We preferred to switch to CTMC calculations using statistics of $N = 100000$ independent electrons for both hydrogenic and microcanonical initial distributions.

We report our total capture cross sections in Fig. 4. In the low energy range ($E = 1$ to ~ 20 keV/amu), our molecular results exhibit an almost flat shape , similar to that found in the classical calculations of Grozdanov (1980) and Perez *et al* (2001). Following our conclusions for Li^{3+} + H collisions, we have included in this figure our CTMC results for impact energies $E \geq 9$ keV/amu, which yield a flat cross section in the low impact energy range, in both hydrogenic and microcanonical calculations. As in Li^{3+} - H collisions, different classical results (Grozdanov 1980, Maynard *et al* 1992, Perez *et al* 2001) and the present one with a microcanonical initial distribution show very good agreement. Nevertheless, the use of this microcanonical distribution ($\mathcal{E} = -0.5$ a.u.) leads to an important underestimation of the total capture cross section for $E \leq 70$ keV/amu. A better description of the outer part of the initial electronic cloud, as provided by the hydrogenic distribution (18), strikingly improves the cross section that then remarkably agrees with its molecular counterpart, which are the reference data at low energies. The comparison of our molecular and hydrogenic CTMC results with the experimental data of Meyer *et al* (1985*a*) is satisfactory.

The use of the hydrogenic distribution also yields a reliable quantitative description of the ionization process (see Fig. 4b), while the microcanonical CTMC calculations underestimate the cross section over the whole impact energy range considered. To check this, and given the lack of alternative experimental or theoretical works, we have

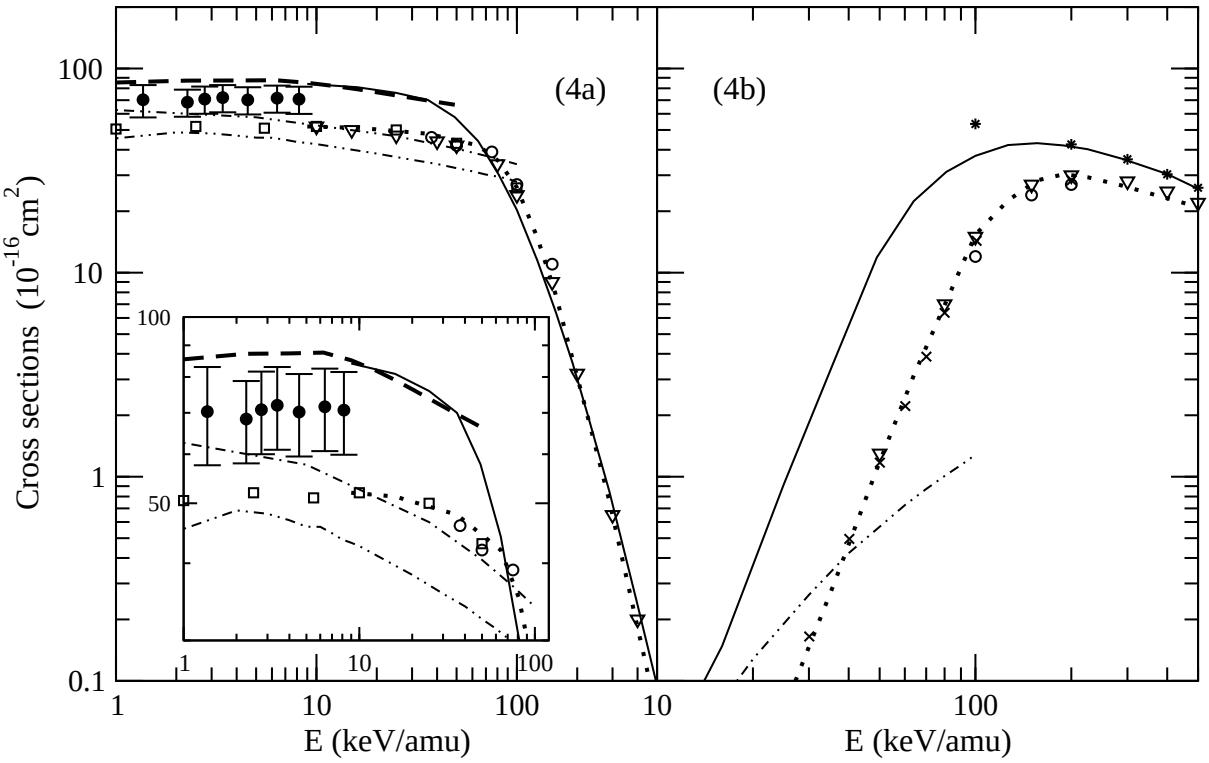

Figure 4. Total capture (a) and ionization (b) cross sections in Ne^{10+}+H(1s) collisions, as functions of the impact energy E. — — — P213 molecular results; Present CTMC results: ——, hydrogenic; · · · ·,microcanonical. Other CTMC calculations: (Grozdanov 1980) (dotted long-dashed line); (◯), (Olson and Salop 1977); (□) (Perez *et al* 2001); ▽, (Maynard *et al* 1992); x, CTMC (Schultz and Krstić 1996). (∗), spherical Bessel monocentric expansion. (- ··), hidden crossing calculations (Schultz and Krstić 1996). Experimental results: ● , (Meyer *et al* 1985*a*).

performed close-coupling calculations in terms of a basis of spherical Bessel functions $j_l(kr)$ confined in a finite box of radius r_{max} centered on the target (Pons 2000, Pons 2001*a*, Pons 2001*b*). The basis includes all the $j_l(kr)$ functions such that $j_l(kr_{max}) = 0$ with $r_{max} = 100$ a$_0$, $0 \leq l \leq 5$ and $0 \leq k \leq 3$ a.u.. The excellent agreement with the hydrogenic CTMC ionization cross section (see Fig. 4b) confirms the accuracy of both sets of results for $E \geq 100$ keV/amu. At lower energies, the hidden crossing calculations of Schultz and Krstić (1996) do not reproduce either our microcanonical or hydrogenic classical results.

We present in Fig. 5 the computed cross sections for capture into the Ne^{9+}(n=5-8)+H^+ shells. In the low impact energy range $E \leq 20$ keV/amu, the molecular results indicate that $n = 6$ and 7 are the main outputs of the capture process whereas our microcanonical CMTC calculations, which are in good agreement with the three-body classical predictions of Olson (1981), Maynard *et al* (1992) and Perez *et al* (2001), lead dominantly to $n = 5$ and 6 and considerably weaken the upper manifold ($n \geq 7$) populations. The hidden crossing calculations of Schultz and Krstić (1996) do not fare

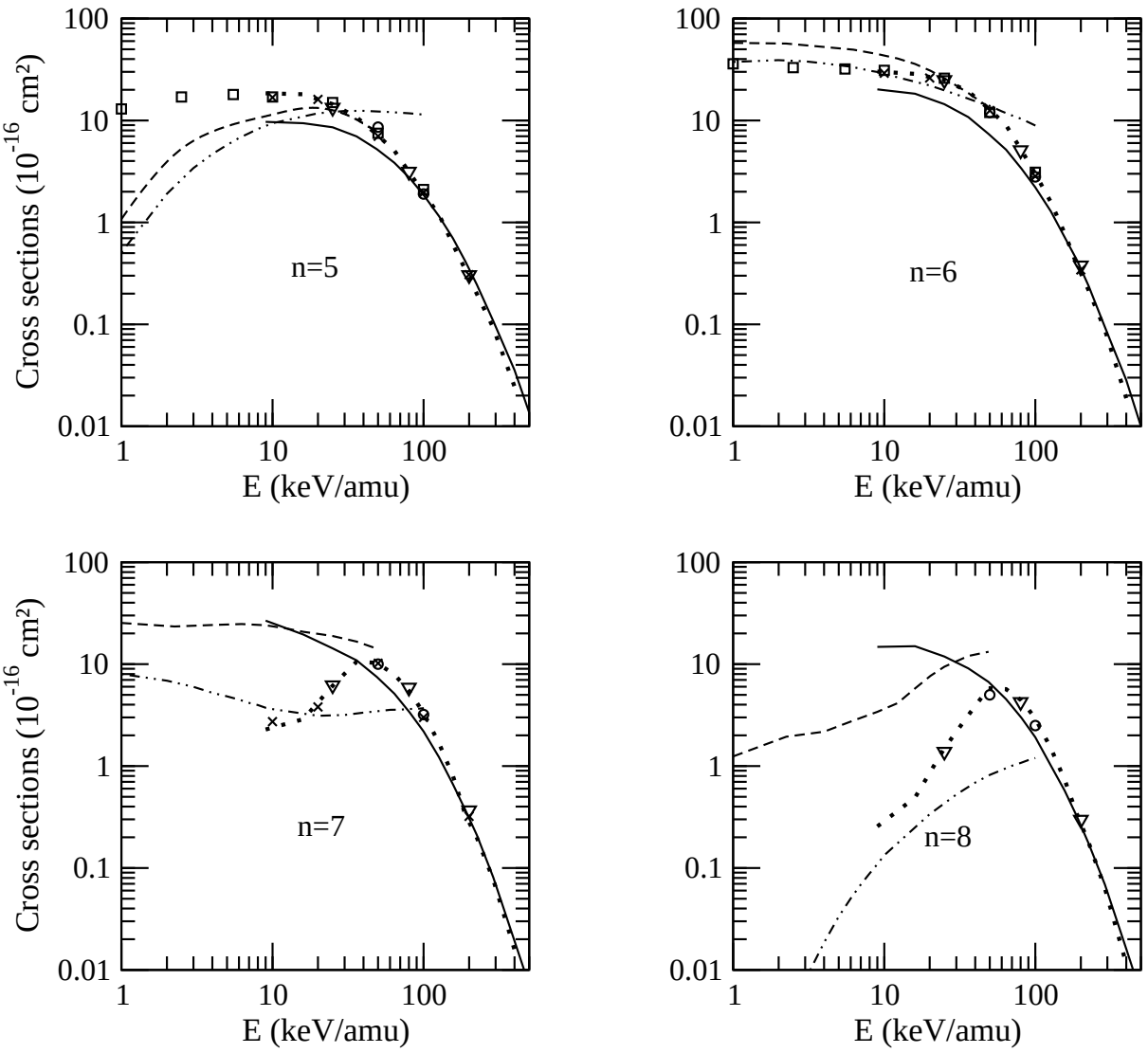

Figure 5. Cross sections for the reactions Ne^{10+}+H(1s) $\longrightarrow$ $Ne^{9+}(n)$+H^+, as a function of the impact energy E. Same symbols as in Fig. 4.

much better than the microcanonical CTMC ones in providing accurate partial cross sections. The classical calculations, with hydrogenic initial distribution, improve the result for the partial cross section to $n = 7$ at low E, but underestimate the cross sections for $n = 5$,6. As the impact velocity increases, the classical results stop exhibiting a strong dependence of the partial cross sections upon the choice of the initial distribution, and suitably coalesce to yield an adequate continuation of the molecular calculations for $E \geq 50$ keV/amu.

In the CXS diagnostic experiments which are actually performed on ASDEX-U, special attention is paid to the Ne X lines associated to radiative transitions in the visible domain ($\Delta n = 1 - 2$) and upper levels corresponding to very excited n states of Ne^{9+}. We thus report in Fig. 6 the hydrogenic CTMC cross sections for capture into

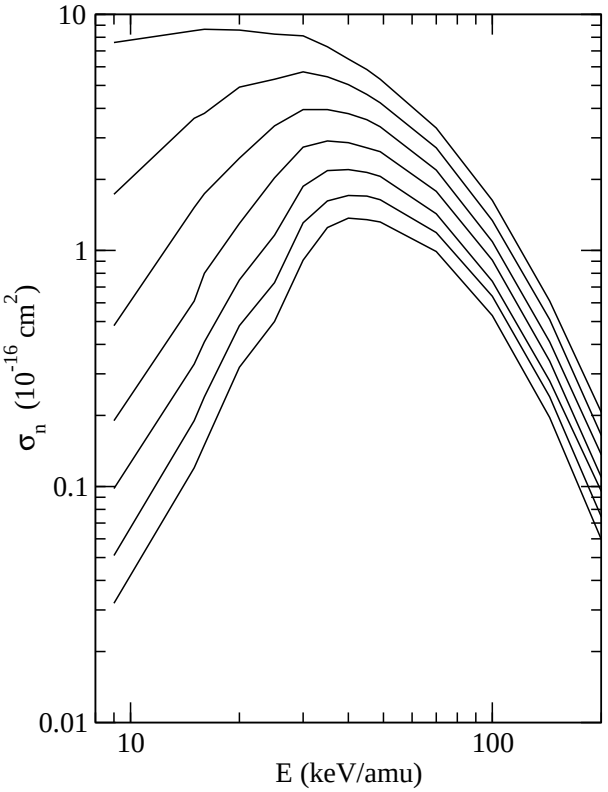

Figure 6. Hydrogenic CTMC cross sections for the reactions Ne^{10+}+H(1s) $\longrightarrow$ $Ne^{9+}(n)$+H^+, with $n = 9$ (top) to 15 (bottom), as a function of the impact energy E.

the $n = 9 - 15$ shells of Ne^{9+}, from $E = 9$ to 200 keV/amu.

We finally consider the l-contributions to the partial n-cross sections, and display in Fig. 7 the ratios σ_{nl}/σ_n, with $5 \leq n \leq 8$ and $0 \leq l \leq n-1$, as functions of E. The most salient feature of Fig. 7 is the overall agreement of the quantum and classical ratios in the intermediate energy range $10 \leq E \leq 50$ keV/amu. Small discrepancies evidently come out for some (n,l) states, as could be expected between two sets of results derived from so distinct methods. Nevertheless, the shape of the ratios always coincide so that one can safely merge the molecular and classical results around 30 keV/amu to provide reliable σ_{nl} capture cross sections over the whole impact energy range of interest for fusion plasma research.

3.3. Continuity between capture and ionization.

The accuracy of the CTMC method in the domain of intermediate impact energies allows an explicit consideration of the continuity between both processes. Continuation across the $E_p = 0$ threshold, with E_p the energy of the electron with respect to the projectile, is a well-known topic (Bransden and McDowell 1992); for instance, it is at the root of the explanation of Rudd and Macek (1972) of the appearance of a conspicuous sharp peak in the ionization cross section in the forward direction by 'charge exchange into the

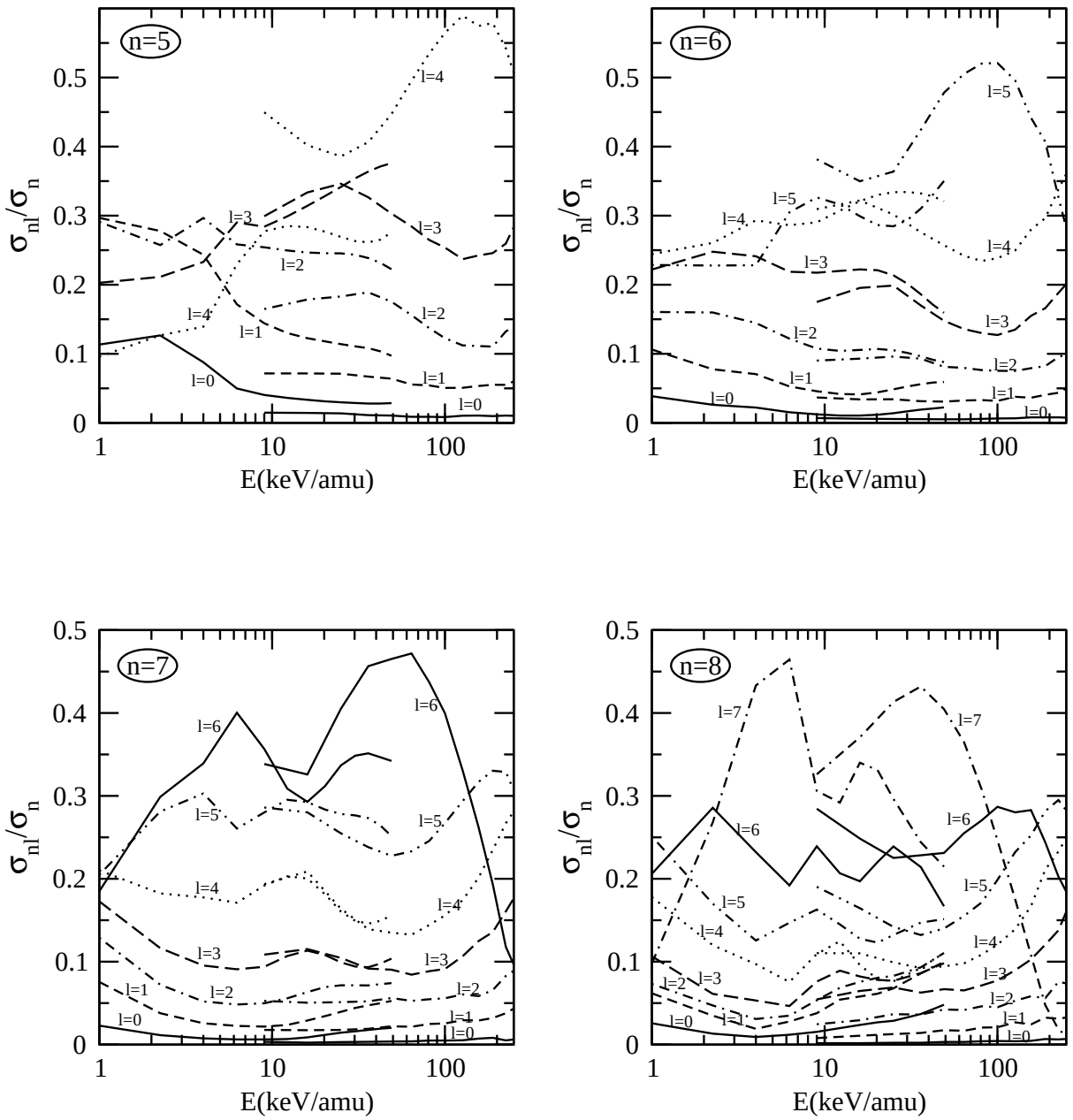

Figure 7. l-contributions to the partial n-capture cross sections in Ne^{10+}+H(1s) collisions, illustrated through the ratios σ_{nl}/σ_n as a function of the impact energy E. Same symbols as in Fig. 4.

continuum'. In particular, elementary considerations assuming continuity between the capture and ionization processes yield the following limit relation between the partial charge transfer σ_n^c and ionization $\sigma_{E_p}^i$ cross sections:

$$\lim_{n\to\infty}\left[\frac{n^3}{Z_p^2}\sigma_n^c(v)\right] = \lim_{E_p\to 0}\sigma_{E_p}^i(v) \tag{22}$$

Assuming that the right-hand-side is nonzero, this leads to the empirical Oppenheimer (Oppenheimer 1928) n^{-3} rule, that is often employed to extrapolate the cross sections

for high n values. We have checked that this law applies to our data at sufficient large nuclear velocities. We note that both the OBK (Oppenheimer 1928, Brinkman and Kramers 1930) and Born 1 (McDowell and Coleman 1970) methods often quoted to justify it are grossly inaccurate for the nuclear velocities treated here.

To display the continuity between capture and ionization, we forego using the Becker-MacKeller binning and define from our classical data a capture cross section $\sigma^c_{E_p}$ that depends on the continuous variable $E_p(< 0)$. We use the same procedure for the ionization cross section, obtaining $\sigma^i_{E_p}$ for $E_p > 0$. We then show in figs. 8a (for Li) and 8b (for Ne) how $\sigma^c_{E_p}$ smoothly join those for $\sigma^i_{E_p}$ at $E_p = 0$ for several impact energies, yielding a combined σ_{E_p} cross section. Further, we mention (but do not show for the sake of clarity) that we obtain for the partial cross sections

$$\sigma^c_n(v) = \frac{Z_p^2}{n^3} \;\; \sigma^c_{E_p}(v) \tag{23}$$

to a very good accuracy.

Next, we notice that in both figures the combined σ_{E_p} cross section exhibits a single maximum, whose position is situated at negative E_p values at low velocities, and increases with v. We then find that when v is high enough that the maximum appears at $E_p > 0$, the empirical n^{-3} rule applies. In fact, since the behaviour of the $\sigma^c_{E_p}$ is then, to a good approximation, exponentially increasing (see figs. 8a,b), we also find that a more accurate empirical expression is given by :

$$\sigma^c_{E_p} \approx K(v) \exp[\alpha(v) E_p] \tag{24}$$

From this, we obtain a corresponding expression for the partial capture cross sections:

$$\sigma^c_n \approx K(v) Z_p^2 n^{-3} \exp[-\alpha(v) Z_p^2/2n^2] \tag{25}$$

that can be applied when the maximum of σ_{E_p} as a function of E_p is located at $E_p > 0$.

We show in figs. 9a (for Li) and 9b (for Ne) the accuracy of this expression for two selected nuclear velocities, with the fitted parameters: K(2) = 2.50, $\alpha(2) = 1.50$, K (1.6) = 9.00, $\alpha(1.6) = 1.733$ for Li^{3+} projectiles and K(2) = 23.8, $\alpha(2) = 1.15$, K(3) = 1.77, $\alpha(3) = 0.87$ for Ne^{10+}, where K is given in units of 10^{-16} cm^2 and α in atomic units. The n^{-3} rule is formally obtained by setting $\alpha = 0$ in these expressions, and is valid for $n \gg Z_p\sqrt{\alpha/2}$, whereas our fitting can be employed for all n.

4. Conclusions

We have calculated, by means of the impact parameter molecular and CTMC methods, total and partial cross sections for capture and ionization in Li^{3+}+H(1s) and Ne^{10+}+H(1s) collisions. The former system, for which several theoretical and experimental data are available, has been studied as a benchmark to ascertain the reliability of the methods in the respective energy ranges where they apply. As a conclusion of the comparison of classical and semiclassical results for capture and ionization in Li^{3+}-H collisions, classical calculations, with improved initial conditions,

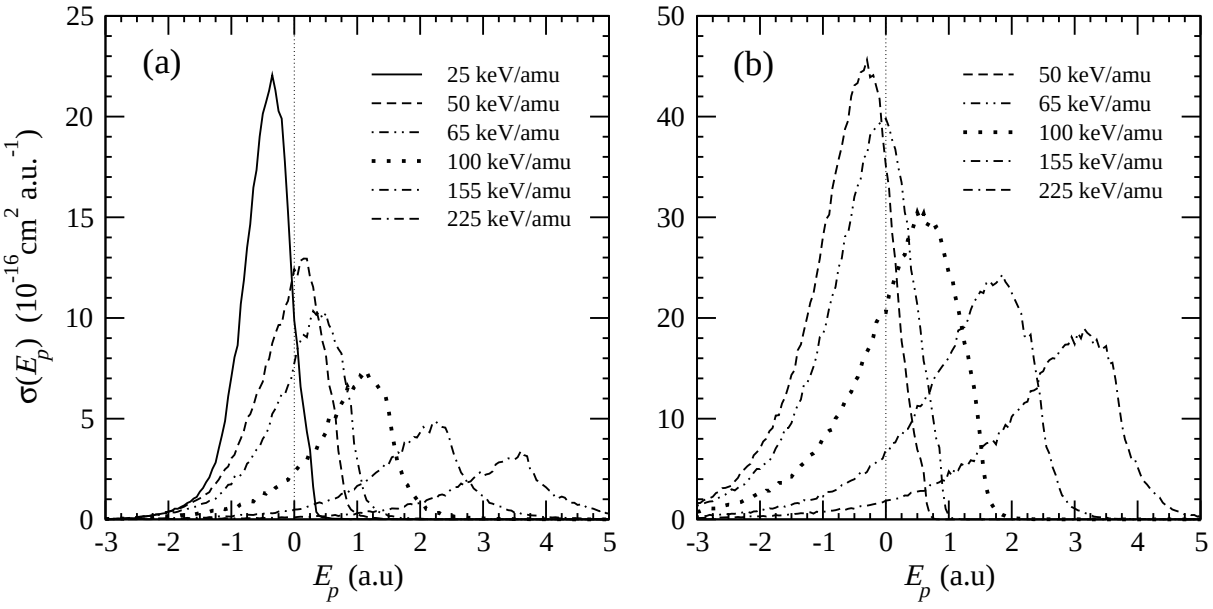

Figure 8. Combined cross section σ_{E_p} for capture and ionization, as defined in text, and as a function of the electronic energy with respect to the projectile E_p at different projectile energies for: (a) Li^{3+}+H(1s) and (b) Ne^{10+}+H(1s) collisions.

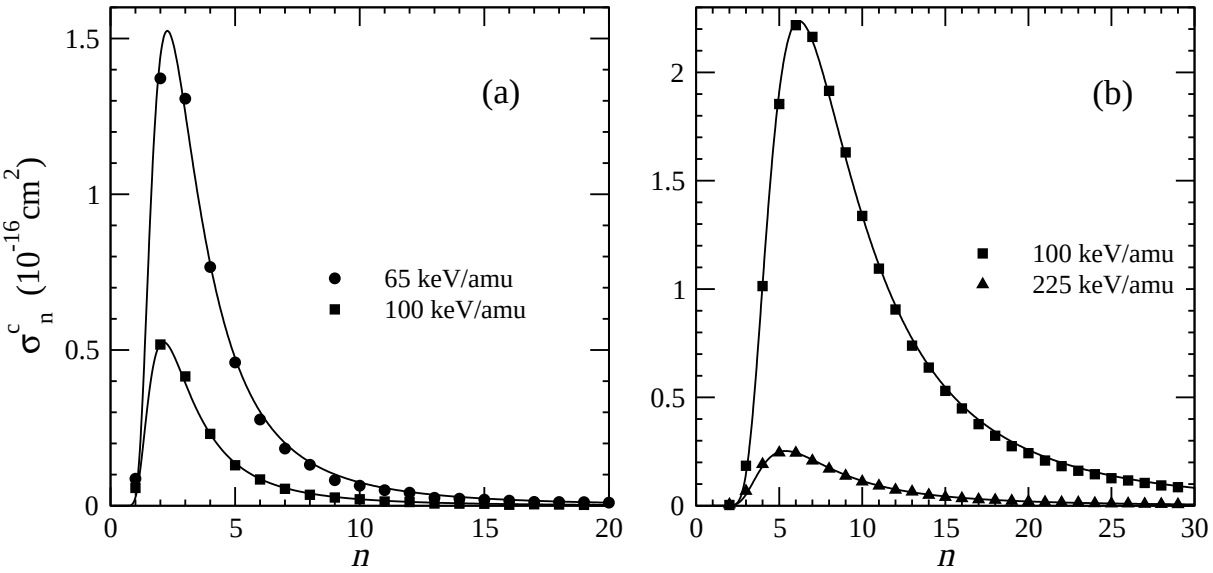

Figure 9. Illustration of the fitting of the partial cross sections σ_n^c by expresion (25). (a) Li^{3+}+H(1s): $\alpha(1.6)$=1.733, K(1.6)=9.00 and $\alpha(2)$=1.50, K(2)=2.50 . (b) Ne^{10+}+H(1s): $\alpha(2)$=1.15, K(2)=23.8 and $\alpha(3)$=0.87, K(3)=1.77 . In both cases, K($v(a.u.)$) is given in units of 10^{-16}cm^2 and $\alpha(v(a.u.))$ in atomic units.

are adequate from high impact velocities down to the maximum of the capture cross section. Some practical guidelines for optimized implementations have emerged from our calculations: in the CTMC method, the use of an initial phase-space distribution that closely mimics *both* the spatial and momentum quantal densities yields a noticeable improvement of the capture and ionization total cross sections. On the other hand, as ionization cross sections are accurately predicted by the CTMC calculations down to low v, it is not indispensable to include pseudostates in the close-coupling molecular treatment insomuch as large-scale expansions in terms of bound molecular orbitals already yields accurate partial capture cross sections up to the maximum of the total capture cross section.

We have then applied our methods to obtain (predictive) values for the capture and ionization cross sections in Ne^{10+}+H(1s) collisions. These data are of crucial importance to consistently analyze the physical state of actual tokamak plasmas in which Ne ionic impurities are deliberately introduced to enhance energy and particle confinement. In the case of such highly charged projectiles, CTMC calculations (Maynard *et al* 1992, Perez *et al* 2001) have been carried from very low (1eV/amu) to high impact energies. However, the comparison with the molecular calculation shows that, as expected, the CTMC does not provide accurate partial capture cross sections at low E and low n values, so that large-scale close-coupling calculations are needed. On the other hand, the CTMC method with the hydrogenic initial distribution, allows to join the low-E molecular results and those obtained at high energies by means of perturbative methods.

ACKNOWLEDGEMENTS

This work has been partially supported by DGICYT projects BFM2000-0025 and FTN2000-0911. We would like to acknowledge the Ministerio de Ciencia y Tecnología (Spain) and the Ministère des Affaires Etrangères (France) for financial support under the coordinated program AIHF04-Picasso2004. C. I. would also like to acknowledge the UAM for support under a research contract.

References

Abrines R and Percival I. C 1966 *Proc. Phys. Soc.* **88** 861

Becker R. L and MacKellar A. D 1984 *J. Phys. B: At. Mol. Phys.* **17** 3923

Belkič D, Gayet R and Salin A 1992 *At. Data Nucl. Data Tables* **51** 76

Bransden B. H and McDowell M. H. C (1992) *Charge Exchange and the Theory of Ion-Atom Collisions* Oxford, Clarendon

Brinkman H. C and Kramers H. A 1930 *Proc. Acad. Sci. Amsterdam* **33** 973

Crothers D. S. F and McCann J. F 1983 *J. Phys. B: At. Mol. Phys.* **16** 3229

Errea L. F, Gorfinkiel J. D, Harel C, Jouin H, Macías A, Méndez L, Pons B and Riera A 1996 *Phys. Scr.* **T62** 33–38

Errea L. F, Harel C, Illescas C, Jouin H, Méndez L, Pons B and Riera A 1998*a* *J. Phys. B: At. Mol. Opt. Phys.* **31** 3199

Errea L. F, Harel C, Jouin H, Maidagan J. M, Méndez L, Pons B and Riera A 1992 *Phys. Rev. A* **46** 5617

Errea L. F, Harel C, Jouin H, Méndez L, Pons B and Riera A 1994 *J. Phys. B: At. Mol. Opt. Phys.* **27** 3603

Errea L. F, Harel C, Jouin H, Méndez L, Pons B and Riera A 1998*b J. Phys. B: At. Mol. Opt. Phys.* **31** 3527

Esipchuk Yu V. *et al.* 2003 *Plasma Phys. Control. Fusion* **45** 793

Folkerts H. O, Bliek F. W, Meng L, Olson R. E, Morgenstern R, von Hellermann M, Summers H. P and Hoekstra R 1994 *J. Phys. B: At. Mol. Opt. Phys.* **27** 3475

Fritsch W and Lin C. D 1982 *J. Phys. B: At. Mol. Phys.* **15** 1255

Gravielle M. S and Miraglia J. E 1995 *Phys. Rev. A* **51** 2131

Grozdanov T. P 1980 *J. Phys. B: At. Mol. Opt. Phys.* **13** 3835

Hardie D. J. W and Olson R. E 1983 *J. Phys. B: At. Mol. Phys.* **16** 1983

Harel C, Jouin H and Pons B 1998 *At. Data. Nucl. Data Tables* **68** 279

Harel C, Jouin H, Pons B, Errea L. F, Méndez L and Riera A 1997 *Phys. Rev. A* **55** 287

Hoekstra R, Anderson H, Bliek F. W, von Hellerman M, Maggi C. F, Olson R. E and Summers H. P 1998 *Plasma Phys. Control. Fusion* **40** 1541

Illescas C and Riera A 1999 *Phys. Rev. A* **A60** 4546

Illescas C, Rabadán I and Riera A 1998 *Phys. Rev. A* **57** 1809

Isler R. C 1994 *Plasma Phys. Control. Fusion* **36** 171

Janev R. K 1989 *Physica Scripta* **T28** 1

Janev R. K 1996 *Physica Scripta* **T62** 1

Le A, Lin C. D, Errea L. F, Méndez L, Riera A and Pons B 2004 *Phys. Rev. A* **69** 062703

Lüdde H. J and Dreizler R. M 1982 *J. Phys. B: At. Mol. Phys.* **15** 2713-2720

Martín F 1999 *J. Phys. B: At. Mol. Opt. Phys.* **32** 501-511

Maynard G, Janev R. K and Katsonis K 1992 *J. Phys. B: At. Mol. Opt. Phys.* **25** 437

McDowell M. R. C and Coleman J. P (1970) *Introduction to the Theory of Ion-Atom Collisions* Amsterdam, North Holland

Meyer F. W, anc C. C. Havener A. M. H and Phaneuf R. A 1985*a Phys. Rev. A* **32** 3310

Meyer F. W, anc C. C. Havener A. M. H and Phaneuf R. A 1985*b Phys. Rev. Lett.* **53** 2663

Olson R 1981 *Phys. Rev. A* **24** 1726

Olson R and Salop A 1977 *Phys. Rev. A* **16** 631

Ongena J. O *et al.* 2001 *Physics of Plasmas* **8** 2188

Oppenheimer J. R 1928 *Phys. Rev.* **31** 349

Perez J. A, Olson R. E and Beiersdofer P 2001 *J. Phys. B: At. Mol. Opt. Phys.* **34** 3063

Pons B 2000 *Phys. Rev. Lett.* **84** 4569

Pons B 2001*a pra* **63** 01274

Pons B 2001*b Phys. Rev. A* **64** 019904(E)

Power J. D 1973 *Phil. Soc. Trans. R. Soc* **274** 663

Rudd M. E and Macek J. H 1972 *Case Stud. At. Phys.* **3** 47

Salin A 1984 *J. Phys (Paris)* **45** 671

Schneiderman S. B and Russek A 1969 *Phys. Rev.* **181** 311

Schultz D. R and Krstić P. S 1996 *At. and Plasma-Material Interaction Data for Fusion* **6** 173

Seim W, Müller A, Wirkner-Bott I and Salzborn E 1981 *J. Phys. B: At. Mol. Phys.* **14** 3475–3491

Sevila I (2003) PhD thesis Universidad Autónoma de Madrid

Shah M. B and Gilbody H. B 1982 *J. Phys. B: At. Mol. Phys.* **15** 413

Shah M. B, Goffe T. V and Gilbody H. B 1978 *J. Phys. B: At. Mol. Phys.* **11** L233

Tokar M. Z, Ongena J, Unterberg B and Weinants R. R 2000 *Phys. Rev. Lett.* **84** 895

Toshima N 1994 *Phys. Rev. A* **50** 3940

Toshima N 1997 *Phys. Scr.* **73** 144

Toshima N 1999 *Phys. Rev. A* **59** 1981